Available online at www.sciencedirect.com
ScienceDirect
Physica A 386 (2007) 212–218
PHYSICA A
www.elsevier.com/locate/physa

Ensemble inequivalence in random graphs

Julien Barré[a,*], Bruno Gonçalves[b]

[a]Laboratoire J.-A. Dieudonné, Université de Nice-Sophia Antipolis, Parc Valrose, 06108 Nice Cedex 02, France
[b]Physics Department, Emory University, Atlanta, GA 30322, USA

Received 15 May 2007; received in revised form 30 June 2007
Available online 15 August 2007

Abstract

We present a complete analytical solution of a system of Potts spins on a random k-regular graph in both the canonical and microcanonical ensembles, using the Large Deviation Cavity Method (LDCM). The solution is shown to be composed of three different branches, resulting in a non-concave entropy function. The analytical solution is confirmed with numerical Metropolis and Creutz simulations and our results clearly demonstrate the presence of a region with negative specific heat and, consequently, ensemble inequivalence between the canonical and microcanonical ensembles.
© 2007 Elsevier B.V. All rights reserved.

PACS: 05.20.−y; 05.70.−a; 89.75.Hc

Keywords: Ensemble inequivalence; Negative specific heat; Random graphs; Large deviations

1. Introduction

When a system phase-separates, it pays for the different domains with a surface energy, which is usually negligible with respect to the bulk energy. In this case, the system is said to be additive: when divided into two macroscopic subsytems, the total energy of the system (or another extensive quantity) is the sum of the energies of the subsystems. As a consequence, any non concave region in the entropy vs. energy curve has to be replaced by a straight line. This is the result of the usual Maxwell construction; this implies for instance that the specific heat is always positive, and that canonical and microcanonical ensembles are equivalent.

However, the condition of additivity or negligible surface energy is violated in presence of long range interactions, as well as for systems with a small number of components. In both cases, the possibility of non concave entropies and ensemble inequivalence is well known, and has been demonstrated on numerous models, for instance [1–4]. The work of Ellis and collaborators have provided some rigorous general results, and shown that the Large Deviation Theory offered the right framework to study the phenomenon [5,6].

In addition to small systems and systems with long range interactions, models on sparse random graphs also violate the condition of additivity: despite the fact that each site has only a small number of neighbors, there will be in general an extensive number of links between two (extensive) subsets of the system. It is thus natural

*Corresponding author. Tel.: +33 4 92 07 62 34; fax: +33 4 93 51 79 74.
E-mail addresses: jbarre@unice.fr (J. Barré), bgoncalves@physics.emory.edu (B. Gonçalves).

0378-4371/$ - see front matter © 2007 Elsevier B.V. All rights reserved.
doi:10.1016/j.physa.2007.08.015

to expect ensemble inequivalences, negative specific heat and other unusual phenomena for these models as well. The possibility of ensemble inequivalence in this type of models has been alluded to in some works related to the statistical physics of random graphs and combinatorial optimization [7]. However, these authors study the analog of the canonical ensemble, and replace the non concave part of the entropy by a straight line. This phenomenon remains thus to our knowledge essentially unstudied, despite the widespread current interest in complex interaction structures, and networks in general. The purpose of this work is to present a simple, exactly solvable model on a random regular network, that displays a non concave microcanonical entropy and ensemble inequivalence. We will show that the recently introduced the Large Deviation Cavity Method (LDCM) [8], coupled with a generalized Legendre transform (defined in Section 2), provides an adequate generalization of the more usual large deviation techniques described for instance in Ref. [5]. This is a first step towards the study of ensemble inequivalence on more complicated networks, which may also include some local structure, like small world networks.

The paper is organized as follows: in Section 2, we present the model, and give its analytical solution, canonical and microcanonical; we then turn in Section 3 to the comparison with microcanonical simulations using both Creutz [9] microcanonical dynamics and Metropolis [10] canonical simulations. The final section is devoted to conclusions and perspectives.

2. Presentation of the model and analytical solution

2.1. The model

We study a ferromagnetic system of Potts spins with three possible states (a, b and c). The Hamiltonian is chosen to be

$$\mathscr{H} = J \sum_{\langle i,j \rangle} (1 - \delta_{q_i q_j}),$$

where $\langle i,j \rangle$ denotes all the bonds in the system, q_i is the state of spin i and $\delta_{q_i q_j}$ is a Kronecker delta. In this form, the Hamiltonian simply counts the number of bonds between spins in different states. The ground state energy is 0. The spins are located on the nodes of a regular random graph where each node has connectivity k, of order 1. A mean field like version of this model, with an all-to-all coupling, displays ensemble inequivalence [3,11].

2.2. Analytical solution

Random regular graphs possess very few loops of size order 1, and locally look like trees; this feature allows us to use standard statistical physics methods, originally developed for Bethe lattices. Solutions of this type of models in the canonical ensemble are classical [12], and we refer to Ref. [13] for a solution of the ferromagnetic Potts model studied here. However, these calculations are usually done in the canonical ensemble only; in contrast, we are interested also in the microcanonical solution. As we want to compute here the microcanonical entropy, which is essentially the large deviation function for the energy, the LDCM described by Rivoire in Ref. [8] is well suited for our problem, and we will make use of this formalism in the following.[1]

We call cavity sites which have only $k-1$ neighbors, and one free link. Cavity site i sends a field h_i along the free link, which tells its state a, b or c. These field are distributed according to the probability distribution $P(h)$:

$$P(h) = p_a \delta_{h,a} + p_b \delta_{h,b} + p_c \delta_{h,c}. \tag{1}$$

Let us now briefly sketch the computation of the microcanonical entropy using the LDCM. Suppose the probability of a spin configuration with energy E, N sites and N_c cavity sites is given by the expression

$$P(E, N, N_c) \asymp \mathrm{e}^{NS(e,r)}, \tag{2}$$

[1]We consider however only large deviation functions with respect to spin disorder, and not with respect to disorder in the graph structure like in Ref. [8]. There is then no conceptual difference between the LDCM and other methods of calculation like the finite temperature cavity method [14].

where $e = E/N$ and $r = N_c/N$; the $\asymp$ symbol denotes that the logarithms of both sides are equivalent. Let us consider a site addition (see Fig. 1, center), causing an energy shift ΔE_{site}, which thus transforms the triplet $(E - \Delta E_{site}, N,\ N_c + k)$ into $(E, N+1, N_c)$. The relation between probabilities before and after the site addition yields

$$\mathrm{e}^{(N+1)S(E/(N+1),N_c/N)} \asymp \int \mathrm{d}\Delta E_{site} \mathrm{e}^{NS(E-\Delta E_{site}/N,(N_c+k)/N)}; \tag{3}$$

this implies (in the limit $r \to 0$):

$$S(e) - \beta e = \ln[\langle \mathrm{e}^{-\beta \Delta E_{site}} \rangle] + kz, \tag{4}$$

where $\beta = \partial S/\partial e\ (e, r = 0)$ (note that β is defined through this relation, and not fixed a priori) and $z = \partial S/\partial r\ (e, r = 0)$. The $\langle\cdot\rangle$ symbol denotes the expected value. We also wrote $S(e)$ instead of $S(e, r = 0)$. Let us consider now a link addition (see Fig. 1, right), causing an energy shift ΔE_{link}, which thus transforms the triplet $(E - \Delta E_{link}, N,\ N_c + 2)$ into $(E, N,\ N_c)$. The relation between probabilities before and after the link addition yields

$$\mathrm{e}^{NS(E/N,\ N_c/N)} \asymp \int \mathrm{d}\Delta E_{link} \mathrm{e}^{NS(E-\Delta E_{link}/N,\ (N_c+2)/N)}; \tag{5}$$

this implies

$$z = -\tfrac{1}{2} \ln[\langle \mathrm{e}^{-\beta \Delta E_{link}} \rangle]. \tag{6}$$

Finally, we note that the function $\beta e - S(e)$ actually depends only on β; we call it the "generalized free energy", and denote it with the symbol $\mathscr{F}(\beta)$. We have the formula

$$\mathscr{F}(\beta) = -\ln[\langle \mathrm{e}^{-\beta \Delta E_{site}} \rangle] + \frac{k}{2} \ln[\langle \mathrm{e}^{-\beta \Delta E_{link}} \rangle]. \tag{7}$$

The analysis of the energy shifts in the $k = 3$ case is detailed in Tables 1 and 2.

The last step is to obtain a self-consistent equation for the probabilities p_a, p_b and p_c through the analysis of the "iteration" process, represented on the left side of Fig 1. During an iteration step, a new site is connected to $k - 1$ cavity sites to become a new cavity site. Several possibilities must be accounted for, corresponding to all the possible configurations along the newly created edges. In Table 3, we represent all the terms to be considered in the $k = 3$ case.

Using this table and following Ref. [8], we obtain:

$$\begin{cases} p_a = \frac{1}{Z}\frac{1}{3}\{p_a^2 + 2p_a(p_b + p_c)\,\mathrm{e}^{-\beta} + (p_b + p_c)^2 \mathrm{e}^{-2\beta}\} \\ p_b = \frac{1}{Z}\frac{1}{3}\{p_b^2 + 2p_b(p_a + p_c)\,\mathrm{e}^{-\beta} + (p_a + p_c)^2 \mathrm{e}^{-2\beta}\} \\ p_c = \frac{1}{Z}\frac{1}{3}\{p_c^2 + 2p_c(p_a + p_b)\,\mathrm{e}^{-\beta} + (p_a + p_b)^2\,\mathrm{e}^{-2\beta}\} \\ Z = \frac{1}{3}\{[p_a + (p_b + p_c)\mathrm{e}^{-\beta}]^2 + [p_b + (p_a + p_c)\,\mathrm{e}^{-\beta}]^2 + [p_c + (p_a + p_b)\,\mathrm{e}^{-\beta}]^2\} \end{cases} \tag{8}$$

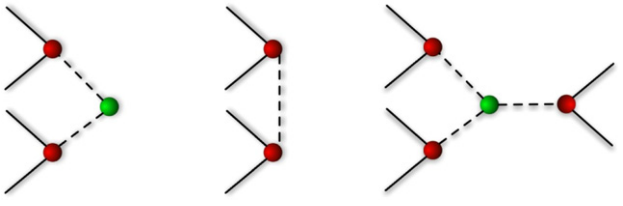

Fig. 1. Schematic representation of the iteration (left), link addition (center) and site addition (right). Red nodes and solid edges represent the original cavity spins and links, while the green colored nodes and dashed lines identify the additions.

Table 1
Configurations (h_1, h_2), energy shifts ΔE and total probabilities $P_l(\Delta E)$ for the case of a link addition

(h_1, h_2)	ΔE	proba.	$P_l(\Delta E)$
(a,a)	0	p_a^2	$p_a^2 + p_b^2 + p_c^2$
(b,b)	0	p_b^2	
(c,c)	0	p_c^2	
(a,b)	1	$2p_a p_b$	$2(p_a p_b + p_a p_c + p_b p_c)$
(a,c)	1	$2p_a p_c$	
(b,c)	1	$2p_b p_c$	

The numeric factors stem from combinatoric arguments.

Table 2
Possible configurations (h_1, h_2, h_3), energy shifts ΔE and probabilities for the different states in which the new site can be

New site	(h_1, h_2, h_3)	ΔE	$P_n(\Delta E)$
a	(a,a,a)	0	$\frac{1}{3}p_a^3$
	$(a,a,b),(a,a,c)$	1	$\frac{1}{3}(3p_a^2 p_b + 3p_a^2 p_c)$
	$(a,b,b),(a,b,c),(a,c,c)$	2	$\frac{1}{3}(3p_a p_b^2 + 3p_a p_c^2 + 6p_a p_b p_c)$
	$(b,b,b),(b,b,c),(b,c,c),(c,c,c)$	3	$\frac{1}{3}(p_b^3 + p_c^3 + 3p_b p_c^2 + 3p_c p_b^2)$
b	(b,b,b)	0	$\frac{1}{3}p_b^3$
	$(b,b,a),(b,b,c)$	1	$\frac{1}{3}(3p_b^2 p_a + 3p_b^2 p_c)$
	$(b,a,a),(b,a,c),(b,c,c)$	2	$\frac{1}{3}(3p_b p_a^2 + 3p_b p_c^2 + 6p_b p_a p_c)$
	$(a,a,a),(a,a,c),(a,c,c),(c,c,c)$	3	$\frac{1}{3}(p_a^3 + p_c^3 + 3p_a p_c^2 + 3p_c p_a^2)$
	(c,c,c)	0	$\frac{1}{3}p_c^3$
c	$(c,c,b),(c,c,a)$	1	$\frac{1}{3}(3p_c^2 p_b + 3p_c^2 p_a)$
	$(c,b,b),(c,b,a),(c,a,a)$	2	$\frac{1}{3}(3p_c p_b^2 + 3p_c p_a^2 + 6p_c p_b p_a)$
	$(b,b,b),(b,b,a),(b,a,a),(a,a,a)$	3	$\frac{1}{3}(p_b^3 + p_a^3 + 3p_b p_a^2 + 3p_a p_b^2)$

The overall factor of $\frac{1}{3}$ corresponds to the *a priori* probability that the new site is in state a and the remaining numeric multipliers stem from combinatorics.

from where we can easily calculate numerically $p_{a,b,c}$. For larger k a straightforward generalizations gives the following equation for p_a, and similar ones for p_b and p_c:

$$p_a = \frac{1}{3Z}[p_a + (p_b + p_c)\,\mathrm{e}^{-\beta}]^{k-1}. \tag{9}$$

Plugging all the previous results into Eq. (7), we obtain the expression of the generalized free energy of the system for the general k case

$$\begin{aligned}\mathscr{F}(\beta) = & -\ln[(p_a^2 + p_b^2 + p_c^2) + 2(p_a p_b + p_a p_c + p_b p_c)\,\mathrm{e}^{-\beta}] \\ & + \frac{k}{2}\ln\left[\frac{1}{3}\{[p_a + (p_b + p_c)\,\mathrm{e}^{-\beta}]^k + [p_b + (p_a + p_c)\mathrm{e}^{-\beta}]^k + [p_c + (p_a + p_b)\,\mathrm{e}^{-\beta}]^k\}\right],\end{aligned} \tag{10}$$

where the three densities p_a, p_b and p_c are solutions of Eq. (9). Notice that this procedure does not necessarily yield the unique "generalized free energy" $\mathscr{F}(\beta)$; rather, there is one value of $\mathscr{F}(\beta)$ for each solution of the consistency equation (9). From the definition of $\mathscr{F}$ and β, it is clear that we must follow all branches of the multi-valued function $\mathscr{F}(\beta)$ to reconstruct the microcanonical entropy $S(e)$ through a generalized inverse Legendre transform (see for instance Refs. [15,16] for a use of this procedure in the context of signal processing)

$$S(e) = \beta e - \mathscr{F}(\beta), \tag{11}$$

Table 3
Analysis of the iteration process for $k = 3$: energy shifts and probabilities

h_0	(h_1, h_2)	ΔE_n	*prob.*
a	(a,a)	0	$\frac{1}{3}p_a^2$
	(a,b)	1	$\frac{1}{3}2p_ap_b$
	(a,c)	1	$\frac{1}{3}2p_ap_c$
	(b,b)	2	$\frac{1}{3}p_b^2$
	(b,c)	2	$\frac{1}{3}2p_bp_c$
	(c,c)	2	$\frac{1}{3}p_c^2$
b	(b,b)	0	$\frac{1}{3}p_b^2$
	(b,a)	1	$\frac{1}{3}2p_bp_a$
	(b,c)	1	$\frac{1}{3}2p_bp_c$
	(a,a)	2	$\frac{1}{3}p_a^2$
	(a,c)	2	$\frac{1}{3}2p_ap_c$
	(c,c)	2	$\frac{1}{3}p_c^2$
c	(c,c)	0	$\frac{1}{3}p_c^2$
	(c,a)	1	$\frac{1}{3}2p_cp_a$
	(c,b)	1	$\frac{1}{3}2p_cp_b$
	(a,a)	2	$\frac{1}{3}p_a^2$
	(a,b)	2	$\frac{1}{3}2p_ap_b$
	(b,b)	2	$\frac{1}{3}p_b^2$

h_0 is the field sent by the new cavity site.

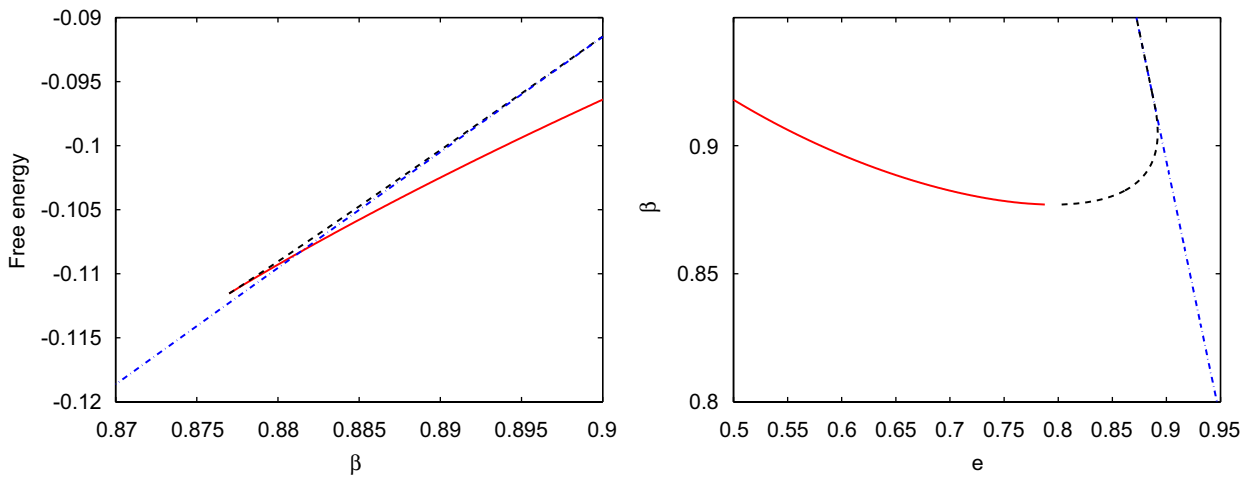

Fig. 2. Left: the three branches of the generalized free energy $\mathscr{F}$ as a function of the inverse temperature β, for $k = 4$. Right: the corresponding three branches for $\beta(e)$ in the microcanonical ensemble.

where

$$e \equiv \frac{\partial \mathscr{F}}{\partial \beta}$$

can easily be calculated numerically using finite differences. This is the final, implicit, solution for the entropy $S(e)$. A comment is in order here: the LDCM naturally yields a multi-valued function $\mathscr{F}(\beta)$, and a generalized Legendre structure. This provides a natural way to compute the microcanonical entropy. This is not always the case with other methods, see Ref. [13].

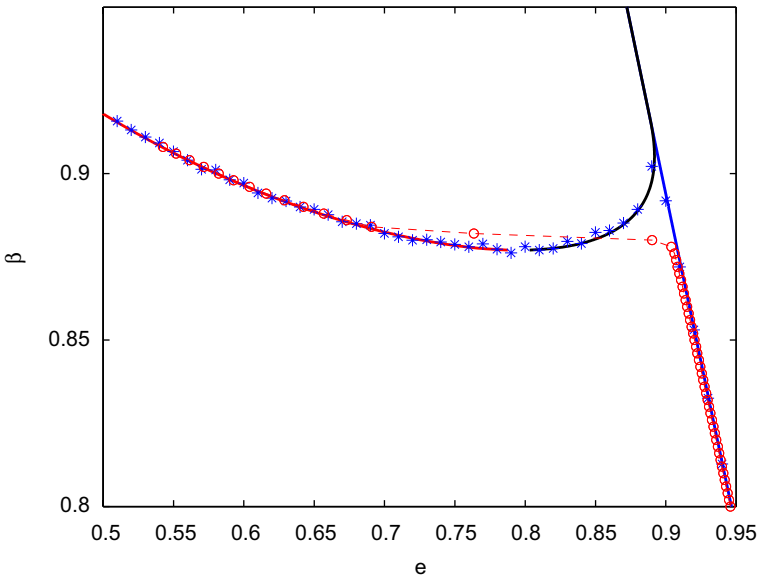

Fig. 3. Comparison for the caloric curve $\beta(e)$ between the analytical solution (solid lines), the Creutz dynamics results (stars), and the Metropolis simulations (circles) for $k = 4$. The Creutz simulations were performed on networks with $N = 40\,000$ sites, for 10^8 "Creutz steps", and the results were averaged over 20 network realizations. The Metropolis results were obtained using 50 different networks with $N = 10\,000$ nodes, by performing 10^{10} Monte Carlo steps. In both cases, the size of the error bars is comparable to the size of the symbols.

In Fig. 2, we plot the different solution branches of $\mathscr{F}(\beta)$, and the inverse temperature $\beta(e)$. One clearly sees a negative specific heat region.

3. Comparison with numerical simulations

In this section we compare the analytical solution with the results obtained through numerical simulations. Microcanonical simulations were performed using Creutz [9] dynamics. During which, a fictitious "demon" is introduced, carrying an energy e_{demon}. At each step, a spin flip in the system is attempted, and the corresponding energy change δE is computed. If $\delta E < 0$, the move is accepted; if $\delta E > 0$, the move is accepted only if $e_{demon} \geqslant \delta E$. In both cases e_{demon} is then updated so that the total energy $E + e_{demon}$ is kept constant; the energy of the system E is then constant up to a $O(1/N)$. For long run times, demon's energy reaches an exponential distribution $P(e_{demon} = e) \propto \exp(-e/T_\mu)$, from where one can compute the corresponding microcanonical temperature $T_\mu = 1/\beta_{mu}$ of our system

$$\beta_\mu = \log\left[1 + \frac{1}{\langle e_{demon}\rangle}\right]. \tag{12}$$

Results of the Creutz dynamics are plotted in Fig. 3 and compared with the analytical solution of the previous section. The agreement between the two is very good, with the β vs. energy curve clearly showing a region of negative specific heat.

Finally, we performed canonical Metropolis [10] simulations and calculated the average energy in the temperature range where our results predict ensemble inequivalence. As expected, the canonical caloric curve obeys Maxwell's construction and clearly "jumps over" the region where the specific heat is negative.

4. Conclusion and perspectives

We have presented a complete canonical and microcanonical solution of the 3-states Potts model on k-regular random graphs, and shown that this toy model displays ensemble inequivalence.

There is little doubt that this result should generically apply to models on different types of random graphs, such as Erdös–Rényi ones, among others. We also expect to observe ensemble inequivalence on small world networks, since in these systems, the presence of random long-range links should prevent the system from separating in two different phases. This provides a whole new family of models with possibly non concave microcanonical entropies, beyond the already well known small systems and systems with long-range interactions.

Beyond the inequivalence between microcanonical and canonical statistical ensemble, non concave large deviation functions should be expected for some properties on random graphs. Fig. 4 of Ref. [7] gives an example of this.

Acknowledgments

The authors would like to acknowledge useful discussions with Stefan Boettcher, Matthew Hastings and Zoltán Toroczkai, and financial support from Grant 0312510 from the Division of Materials Research at the National Science Foundation.

References

[1] P. Hertel, W. Thirring, Soluble model for a system with negative specific heat, Ann. Phys. 63 (1971) 520.
[2] D.H.E. Gross, Microcanonical Thermodynamics: Phase Transitions in Small Systems, Lecture Notes in Physics, vol. 66, World Scientific, Singapore, 2001.
[3] I. Ispolatov, E.G.D. Cohen, On first-order phase transitions in microcanonical and canonical non-extensive systems, Physica A 295 (2001) 475.
[4] J. Barré, D. Mukamel, S. Ruffo, Inequivalence of ensembles in a system with long range interactions, Phys. Rev. Lett. 87 (2001) 030601.
[5] R.S. Ellis, The theory of large deviations: from Boltzmann's 1877 calculation to equilibrium macrostates in 2D turbulence, Physica D 133 (1999) 106.
[6] R.S. Ellis, K. Haven, B. Turkington, Large deviation principles and complete equivalence and nonequivalence results for pure and mixed ensembles, J. Stat. Phys. 101 (2000) 999.
[7] A. Engel, R. Monasson, A. Hartmann, On large deviation properties of Erdös–Rényi Random Graphs, J. Stat. Phys. 117 (2004) 387.
[8] O. Rivoire, The cavity method for large deviations, J. Stat. Mech. P07004 (2005).
[9] M. Creutz, Microcanonical Monte Carlo simulation, Phys. Rev. Lett. 50 (1983) 1411.
[10] N. Metropolis, A.W. Rosenbluth, M.N. Rosenbluth, A.H. Teller, E. Teller, Equation of state calculations by fast computing machines, J. Chem. Phys. 21 (1953) 1087.
[11] M. Costeniuc, R.S. Ellis, H. Touchette, Complete analysis of phase transitions and ensemble equivalence for the Curie–Weiss–Potts model, J. Math. Phys. 46 (2005) 063301.
[12] R.J. Baxter, Exactly Solved Models in Statistical Mechanics, Academic Press, New York, 1982.
[13] D.A. Johnston, P. Plecháç, Potts models on Feynman diagrams, J. Phys. A 30 (1997) 7349.
[14] M. Mézard, G. Parisi, The Bethe lattice spin glass revisited, Eur. Phys. J. B 20 (2001) 217.
[15] M.J. Sewell, On Legendre transformations and elementary catastrophes, Math. Proc. Cambridge Philos. Soc. 82 (1977) 147.
[16] P. Maragos, Slope transforms: theory and applications to non linear signal processing, IEEE Trans. Signal Process. 43 (1995) 864.